Geomechanics and Engineering, *Vol. 31, No. 3 (2022) 305-318*
https://doi.org/10.12989/gae.2022.31.3.305

An assessment of the mechanical behavior of zeolite tuff used in permeable reactive barriers

Gökhan Çevikbilen*

Department of Civil Engineering, Istanbul Technical University,
ITU Ayazaga Campus, Faculty of Civil Engineering, Room 140413, Sarıyer, 34469, Istanbul, Turkey

(*Received October 24, 2021, Revised October 29, 2022, Accepted October 30, 2022*)

Abstract. Permeable reactive barriers used for groundwater treatment require proper estimation of the reactive material behavior regarding the emplacement method. This study evaluates the dry emplacement of zeolite (clinoptilolite) to be used as a reactive material in the barrier by carrying out several geotechnical laboratory tests. Dry zeolite samples, exhibited higher wetting-induced compression strains at the higher vertical stresses, up to 12% at 400 kN/m^2. The swelling potential was observed to be limited with a 3.5 swell index and less than 1% free swelling strain. Direct shear tests revealed that inundation reduces the shear strength of a dry zeolite column by a maximum of 10%. Falling head permeability tests indicate decreasing permeability values with increasing the vertical effective stress. Regarding self-loading and inundation, the porosity along the zeolite column was calculated using a proposed 1D numerical model to predict the permeability with depth considering the laboratory tests. The calculated discharge efficiency was significantly decreased with depth and less than 2% relative to the top for barrier depths deeper than 20 m. Finally, the importance of directional dependence in the permeability of the zeolite medium for calibrating 2D finite element flow analysis was highlighted by bench-scale tests performed under 2D flow conditions.

Keywords: clinoptilolite; hydro-compression; permeability; permeable reactive barrier; shear strength; zeolite

1. Introduction

Remediation of contaminated groundwater is a major environmental issue at contaminated sites (IAEA 1999). Permeable reactive barrier (PRB) technology is being introduced as an alternative method for controlling and treating groundwater, contaminated with heavy metals (Ludwig *et al.* 2002), chlorinated organics and radionuclides, etc. (ITRC 2005). To keep the cost of PRB technology to a minimum while also in line with regulatory decontamination requirements for the contaminants (USEPA, 2002), the reactive media should be readily available at a low to moderate cost (Gavaskar 1999, Morrison *et al.* 2003).

When the contaminated groundwater passes through the manmade permeable barrier layer placed in the soil profile, pollutants are degraded or stabilized. Zero valence iron (Henderson and Demond 2007, Korte 2001, Wang and Zhang 1997), activated carbon (Bone 2012), oxides (Navarro *et al.* 2006,), lime and other alkaline materials (Thiruvenkatachari *et al.* 2008), aerobic or anaerobic biodegradation materials for biobarriers (Walker *et al.* 2020), organoclay, or zeolite (Vignola *et al.* 2011) are among the reactive materials preferred for use in PRB implementations. The weight of reactive material per unit cross-section of the plume has important implications in terms of the choice of permeable barrier design and emplacement method (USEPA 2002). The use of tremie tubes, trenching machines, high- pressure jetting, and deep soil mixing approaches may be appropriate for different situations, depending on the amount of reactive material required, the dimensions of the plume, and other factors (Powell *et al.* 1998). Furthermore, the required residence time of the plume within the reactive media and the local hydrogeological conditions typically dominate the selection of the dimensions and location of the barrier. PRBs can be oriented horizontally as compacted layers or vertically in continuous trenches or funnel and gate systems (Bowles *et al.* 2000), depending on the contamination scenario in their region of use. In a common use of vertical PRBs, hanging or keyed-in competent aquitard types can be applicable against the low density polyethylene LDPE or high density polyethylene HDPE, respectively.

The feasibility and performance of a barrier design should satisfy the requirements of environmental and geotechnical safety regulations, which can be tested using numerical analysis, supported by laboratory and in-situ testing (ITRC 2005). Hydrogeological models are used to assess contamination scenarios due to overflow, under-flow, or flow across the barrier under steady-state and transient flow conditions (i.e., Naidu and Birke 2015). The consistency in hydraulic conductivity between the soil layers and the barrier plays an essential role. If a reactive material is selected that is impervious relative to its surroundings, this can potentially cause the contaminant to bypass the PRB. Therefore, laboratory-based hydraulic conductivity tests on reactive media under in-situ stress levels are required to verify that permeability of the barrier is equal to or slightly higher than the surrounding layers, as

*Corresponding author, Ph.D.
E-mail: cevikbil@itu.edu.tr

ISSN: 2005-307X (Print), 2092-6219 (Online)

is most commonly needed. Furthermore, the short and long term stability conditions of PRBs should be analyzed in the context of the emplacement methodology related to the site-specific, soil, pollutant and hydrogeological conditions. Replacement of reactive materials during the lifespan of a PRB may be required in an unpredictable scenario such as climate change or acid rain if the threshold allowance limit for a pollutant overflows. Therefore, studies on the use of locally available sources of alternative reactive materials are crucial for the cost-effective and timely emplacement and replacement of PRBs.

Korte (2001) reported that loss of hydraulic conductivity in PRBs may be due to construction-induced compaction for coarse-grained soils or smearing effects on the soils with high clay content during trenching or sheet pile driving. Additionally, Symth (1995) noted that the problems in packing reactive materials may cause poor PRB performance. Therefore, the effects of the as-built conditions of the reactive material columns, before their usage for treatment, on the performance of PRBs need to be investigated in detail.

Most previous studies have focused on the choice of raw or synthetic reactive material and its longevity against contaminants (e.g., Bagherifam *et al*. 2021, Ghiyas and Bagheripour 2020, Vignola *et al.* 2011). On such material is naturally occurring zeolite, which consists of linked SiO4 and AlO4 and has a potential to be used as an alternative reactive material for PRBs in Turkey. Zeolites behave as a molecular sieve and ion exchanger and have a variety of applications such as agriculture, health, and air or water treatments after physical or chemical conditioning.

The mechanical and hydraulic behavior of zeolite change significantly related to the emplacement method applied for the geoenvironmental problems. The use of zeolite and zeolite/bentonite mixtures as soil-based materials in compacted layers for the capping of landfills or in slurry walls were examined for the containment of contaminated soil and groundwater (Kayabalı and Kezer 1998, Tuncan *et al.* 2003, Oren *et al*. 2011, Oren and Kaya 2014, Joseph and Varghese 2019, Widomski *et al.* 2021). Ören and Özdamar (2013) presented that the hydraulic conductivity of the compacted zeolite under standard energy is in the range of 5.2×10^{-5} and 1.1×10^{-9} m/s, and varies with the particle size, initial moisture content and pore volumes of flow. The rigid wall hydraulic conductivity tests revealed that the hydraulic conductivity values of granular zeolites were two orders of magnitude higher than fine zeolites. Meanwhile the hydraulic conductivities of the samples, compacted at the water content on the dry side of the optimum, was at least one and two orders of magnitude higher than the samples prepared at the wet of optimum for granular and fine zeolite, respectively. It was concluded that hydraulic conductivity of the compacted zeolite, mainly controlled by the fine content up to a value of 39% was not adequate for the liner or cap layers.

In PRB implementations, the higher values of hydraulic conductivity can be achieved when the grain size distribution of zeolite is adjusted by limiting the fine fraction or by increasing the coarse fraction through the addition of sand. Park (2002) studied on the mixtures of clinoptilolite-type zeolite and Jumunjin sand with a ratio of 20:80 by weight to be used as a reactive material in PRB for the treatment of ammonium, lead, and copper. In that study, hydraulic conductivity of the barrier was modelled by flexible wall permeameter under a confining pressure at about 70 kN/m^2 equals to the overburden pressure. It was found that low hydraulic conductivity values of 100% zeolite (1×10^{-8} m/s) was increased to 1×10^{-6} m/s when the mean particle size of zeolite was similar to sand in the mixture.

When the required height of the PRB increases, the assumption of an average value for hydraulic conductivity to evaluate the remediation efficiency of the barrier will not be realistic. Therefore, the relationship between overburden stress-porosity-hydraulic conductivity of zeolite used along the barrier should be studied by considering the emplacement method and in-situ conditions. In the literature the emplacement of dry raw clinoptilolite into the gates of PRB keyed in competent aquitards has not been adequately discussed in which the inundation may result internal instability (i.e., swell or collapse) or the self-weight consolidation behavior causes a loss in hydraulic conductivity.

In this study, we evaluate the emplacement of a clinoptilolite-type zeolite tuff used as an alternative reactive material in the trench of vertical PRBs. Zeolite finer than the 1 mm fraction was used in its dry state. In addition to the index properties of zeolite, i.e., the consistency limits, and grain size distribution, the swell or collapse behavior of the column was also examined using samples prepared under several stress levels. Changes in the shear strength of zeolite due to inundation are also presented. The influence of changes in effective stress on hydraulic conductivity was investigated using one-dimensional consolidation and falling head-type permeability tests, which demonstrated that the porosity (n), defined by the ratio of volume of voids in a unit volume of reactive material, mainly controls the permeability of the zeolite in both virgin compression and reloading stages. Therefore, a one-dimensional numerical compression model was proposed to characterize the change in the porosity, by self-loading and wetting-induced compression through the zeolite column, which was then used to determine the permeability with depth. Two-dimensional bench-scale flow tests were used to calibrate the model parameters of a 2D finite element flow analysis; these tests showed that the directional dependency of flow on the hydraulic conductivity of zeolite requires further examination to prevent the improper design of PRBs.

2. Materials

Nuclear power plants are being constructed in Turkey due to the increase in energy consumption triggered by growth in the country's population and industries, thus, local storage facilities for low-level radioactive wastes will be required. Potential storage sites should, therefore, be investigated for the containment and treatment of soil and groundwater contamination through the use of cost-effective, local resources as reactive materials. Isotopes such as Sr, Cs, Co, and Ca, which are found in nuclear

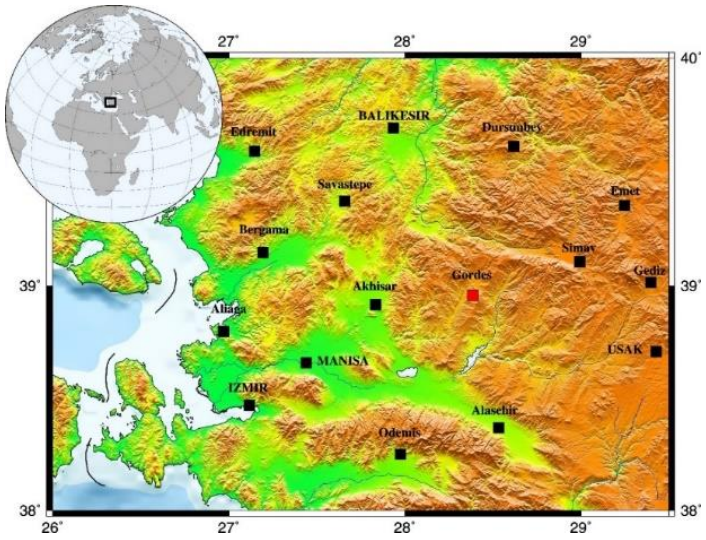

(a) Gördes: Location of zeolite source. Topography and bathymetry data are taken from NASA-SRTM3 and Smith and Sandwell (1997a, b), respectively

(b) Raw zeolite

(c) Granulated raw zeolite

Fig. 1 The source of zeolite samples used in the study

Table 1 Physical properties of materials defined by this study following the relevant methods (ASTM)

Properties	Zeolite	Sand	Method
Sand size fraction (%) [2-0.075mm]	67	100	ASTM D6913
Silt size fraction (%) [0.075-0.002mm]	29	0	ASTM D7928
Clay size fraction (%) [<0.075mm]	4	0	ASTM D7928
Liquid Limit, w_L (%)	58	-	ASTM D4318
Plastic limit, w_P (%)	39	-	ASTM D4318
Plasticity Index, I_P (%)	19	NP	ASTM D4318
USCS Soil Type	SM	SP	ASTM D2487
Maximum void ratio, e_{max}	1.59	0.80	ASTM D4254
Minimum void ratio, e_{min}	1.09	0.57	ASTM D4253
Specific Gravity G_s	2.35	2.67	ASTM D854
Swelling Index (mL/2g)	3.5	-	ASTM D5890

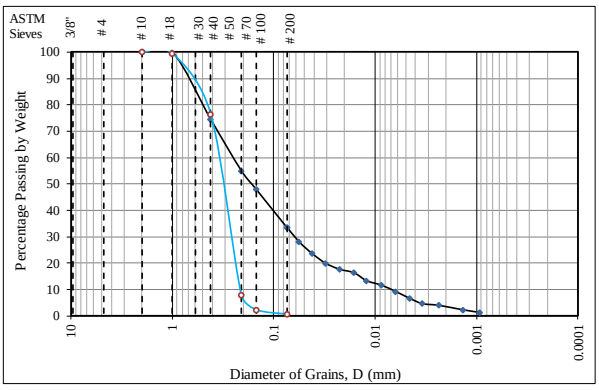

Fig. 2 Grain size distribution of zeolite (black) and sand (blue)

power plant waste, can be retained with zeolites. Notably, Turkey has rich resources of zeolite in the Aegean, Central Anatolia and Eastern Anatolia regions (MTA 2021). Kütük *et al*. (1996) described rheological observations of the zeolite tuffs of the Manisa region (Figs. 1(a) and 1(b)) is clinoptilolite which has a better cation capacity, MB spot specific surface area (Aksoy 2010). In this study, a local zeolite supplier (Gördes zeolite company) was chosen for clinoptilolite in the form of commercially available solid powder with a light cream color and less than 1.0 mm diameter (Fig. 1(c)). The mineralogical composition of the samples, as determined by the X-Ray fluorescence analysis standard DIN51001, is provided in the Appendix (see Table A.1).

The index properties of the soil-based materials used in this study (i.e., zeolite, and sand) were determined according to the relevant ASTM standards. Their grain size distributions are plotted as in Fig. 2. Soil type based on Unified Soil Classification System and other physical properties of the samples were summarized in Table 1. The swelling index of silty sand (SM) type zeolite samples was also tested. The surface area NH_4^+ content, thermal stability, and water retention capacity values of clinoptilolite are presented in the Appendix (see Table A.2) as given by the supplier's datasheet.

Fig. 3 Geocomp Trac II direct shear test device used in the study

(a) ELE Rowe cell

(b) ELE odeometer cell and frame

(c) Trautwein buble tube permeameter

Fig. 4 Some of the laboratory test settings used in the study

3. Methods

The swell or collapse tests were conducted as described in the ASTM D4546 method. Eight dry zeolite specimens, each 6.35 cm in diameter and 2.87 cm in height, were reconstituted in the unconsolidated state. Wetting-after-loading type tests were performed by inundation each of the specimens after incrementally loaded to a predesignated vertical effective stress (σ'_v) in between 1 and 400 kN/m². Time-dependent vertical deformation (ε_v) of the specimens was recorded throughout the tests. In addition, the free swelling behavior of zeolite was investigated on a specimen under contact pressure equal to 1 kN/m². After the primary swelling test, the specimen was subjected to further loading up to 400 kN/m² incrementally to illustrate the post-compression behavior.

The shear strength of the zeolite at different fill depths of the gate was investigated on multiple reconstituted specimens using a direct shear test device shown in Fig. 3. Seven dry zeolite specimens of 6.35 cm diameter and 2.85 cm height were initially reconstituted in the cell in the loosest state. Incremental loading was applied at a unit load increment ratio (LIR) value of 1, up to a final σ'_v equal to 12.5, 25, 50,100, 200, 300, or 400 kN/m². Load increment durations (LID) were sufficiently long to finalize the compression. When the vertical displacements were stabilized at $\sigma'_{v\,final}$, the cell housing was filled with water to saturate the specimen from bottom to top through the porous stones placed at its upper and lower boundaries. When the primary swell or hydro compression deformation had been completed according to method A in ASTM D4546, the specimens were sheared at a constant rate of lateral displacement that satisfies the drained conditions stated in ASTM D3080. In addition, the tests were also conducted on the reconstituted samples with the same loading program without the saturation process to compare the findings with the shear strength of zeolite in the dry state.

One dimensional consolidation tests were conducted on zeolite samples by using incremental loading in a front loading-type consolidation frames. The reconstituted samples were prepared with an initial water content equal to 1.5 times the liquid limit at σ'_v, equals to 25 kN/m², in a small Rowe cell (Fig. 4(a)). Conventional consolidation testing was performed in accordance with the ASTM D2435 specification (Fig. 4(b)). The test specimen, placed in the stainless steel ring was in the dimensions of 2 cm thick and 7.5 cm diameter. Two-way drainage was allowed through the porous stones placed at the upper and lower boundaries. An LIR of 1 was applied with loading values of 25, 50, 100, 200, 400 and 800 kN/m² and LID was at least 24 hours. The ε_v values were observed by using linear variable differential transformers throughout the test.

The vertical permeability of the reactive media at various column depths was modelled in an odeometer cell, specialized for permeability tests (Fig. 4b). Falling head-type permeability tests were conducted after the end of primary consolidation under σ'_v values equals to 25, 50, 100, 200, 400 and 800 kN/m^2 after fixing the loading yoke that prevented further displacements throughout each test. The tests were also repeated at the unloading stage of each loading step after the end of primary swelling.

A bench-scale PRB configuration was designed to investigate the 2D flow of groundwater during steady-state flow conditions, as shown in Fig. 5. A Plexiglas box was constructed with the adjustments made for several model setups. The PRB was modelled using a 1.0 cm thick zeolite barrier in the flow direction with a vertical cross-sectional

Fig. 5 Bench scale PRB configuration designed for modelling 2D flow in reactive media

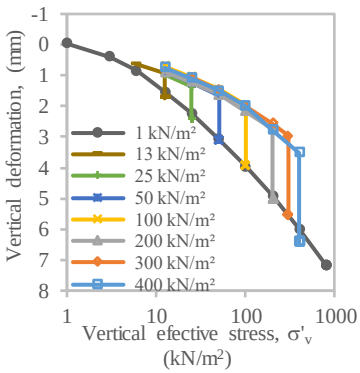

(a) Compression curves of swell or collapse tests

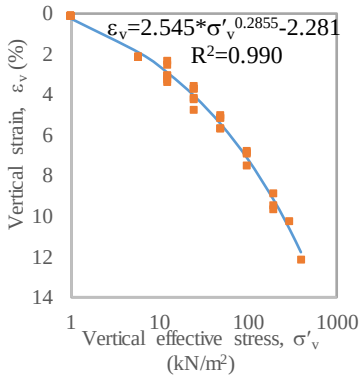

(b) Predicted compression curve of dry zeolite

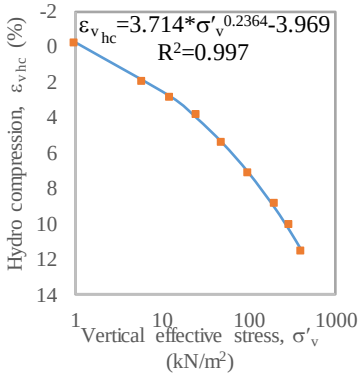

(c) Predicted hydro-compression curve of dry zeolite

Fig. 6 The results of swell or collapse tests

area of 3.5 x 9.0 cm^2. The granular soil media used in the gate of the PRB systems was simulated by a sand fill at the effluent side. A constant head-type permeability test was conducted in accordance with the ASTM D2434 on the sand sample by using a bubble tube-type permeameter. Relative density tests were performed on the dry sand to calculate the unit weight that corresponds to a 65% relative density value, to be used in modeling as an initial state. A non-woven geotextile with an apparent opening size of 0.076 mm was used as a separator fixed between the reactive and soil media (for details, see Camtakan 2021). The permittivity value of the geotextile was 65 l/s.m^2, therefore, the head loss through the geotextile was assumed negligible. The predetermined dry unit weight requirement is satisfied by placing the calculated weights of each medium for the proposed volume values between the separators, which were initially laterally supported. Inundation was applied for more than a week to satisfy the full saturation condition; the proposed constant head difference between the downstream and upper stream was then arranged in the model. The measurement techniques employ the Mariotte's bottle apparatus and a passive siphon system to provide constant head values at both the influent and effluent sides. The time-dependent change in the total volume of water that passed through the model was observed at the influent and effluent sides by measuring either the reduction of the water level in a graduated tube or the collected volume in a jar. The test was repeated several times. Evaporation was prevented during the test with a transparent cover that the model box does not come into direct contact with.

4. Laboratory test results

4.1 One dimensional compression tests

The one-dimensional compression behavior of the zeolite column was examined both before and after inundation using the swell and collapse and conventional consolidation tests (Figs. 6 and 7). The amount of free swelling of dry zeolite under σ_v equal to 1 kN/m² was observed to be negligible (<0.3 %). The compression curve of the sample loaded after free swelling is shown in Fig. 6(a) with solid line circle markers. The wetting-induced swell or collapse behaviors of dry zeolite samples were observed at seven different σ'_v values as given in Fig. 6(a), which shows the compression curves of the samples before inundation. A power trend line was identified with a corresponding R^2=0.99 (Fig. 6(b)), represent the vertical deformation versus σ'_v of the dry samples. The goodness of fit value indicates that the initial reconstitution conditions of the samples in their loosest state were sufficient and of good quality. The wetting induced strain versus σ'_v curves plotted separately in Fig. 6(c) show higher hydro compression ratios $\varepsilon_{v\,hc}$ at higher values of σ'_v. A unique hydro compression curve of dry samples after inundation was generated with a power trend line corresponding to R^2=0.99 as illustrated in Fig. 6(c).

The σ'_v versus void ratio (e) graph from the oedometer test is plotted in Fig. 7(a) to illustrate the one-dimensional behavior of the saturated zeolite column. The compression index C_c and secondary compression index C_α values are

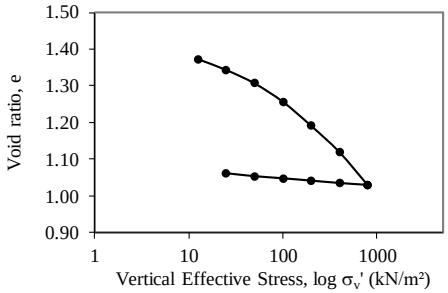

(a) Compression curve

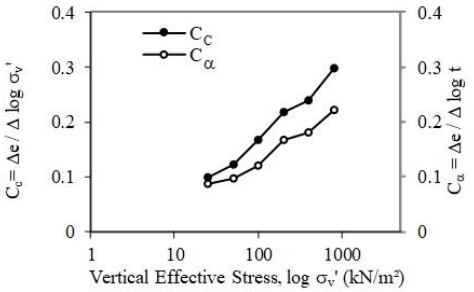

(b) The compression indexes at the stress levels

Fig. 7 Consolidation test results of saturated zeolite

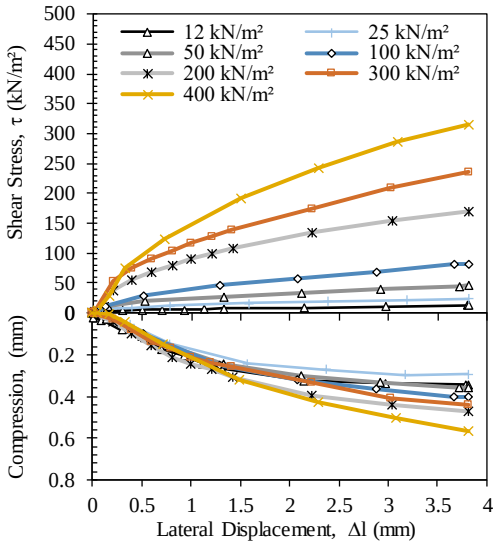

(a) The observed data of dry zeolite by time

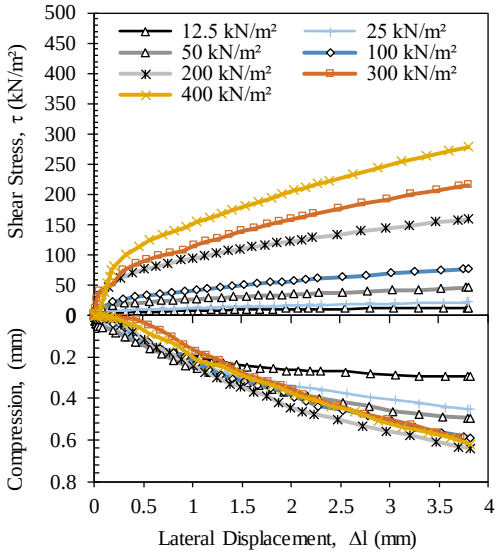

(b) The observed data of inundated zeolite by time

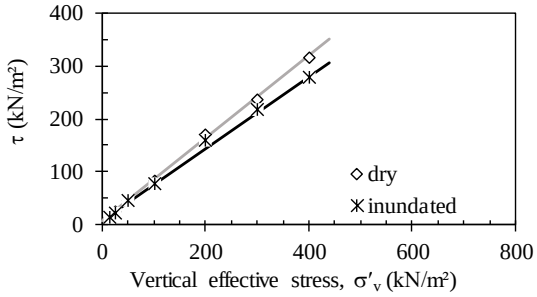

(c) Shear failure envelopes for dry and inundated zeolite

Fig. 8 Direct shear test results of zeolite

shown in Fig. 7(b) in terms of the consolidation pressure values. The ratio of C_c/C_α above the reconstitution pressure is observed to be equal to 4.42. The secondary compression coefficient $C_{\alpha\varepsilon}$, calculated to be the C_α value normalized by $(1+e_0)$ has a value between 0.2 and 0.8% indicating that the zeolite sample can be classified as having low to medium secondary compression potential (Mesri 1973).

4.2 Shear strength tests

The shear strength of dry zeolite samples was compared with inundated samples at seven different values of σ'_v. Figs. 8(a) and 8(b) presents the shear stress and vertical deformation versus the lateral displacement observed in the direct shear tests of dry and inundated zeolite samples, respectively. The shear strength angle (ϕ), and cohesion (c), parameters were determined as ϕ=38° and c=6 kN/m^2 for dry zeolite samples, and ϕ=35° and c=8 kN/m^2 for zeolite samples after inundation (Fig. 8(c)). These findings are in the range of shear strength parameters determined by Villalobos *et al.* (2018) for the fine sand and silt particle size zeolite samples prepared at 30 % relative density.

The shear strength values of dry and inundated zeolite samples normalized by σ'_v were observed to be lower at

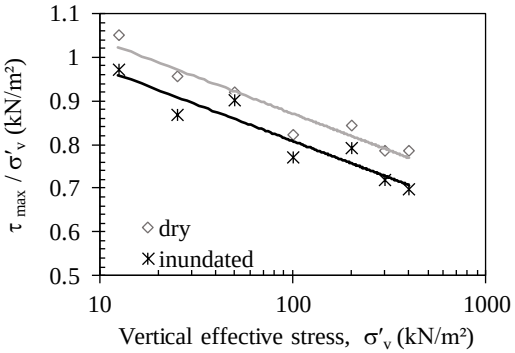

(a) Normalized shear strength values of zeolite

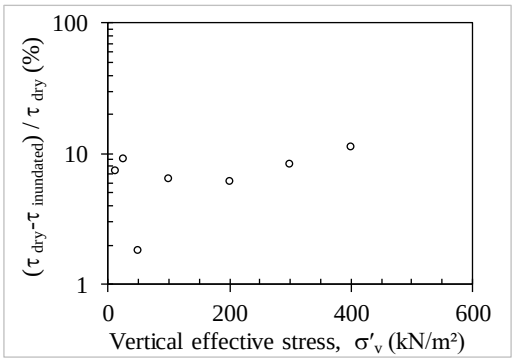

(b) The change in shear strength due to inundation

Fig. 9 Comprasion on the shear strengths of inundated and dry zeolite samples

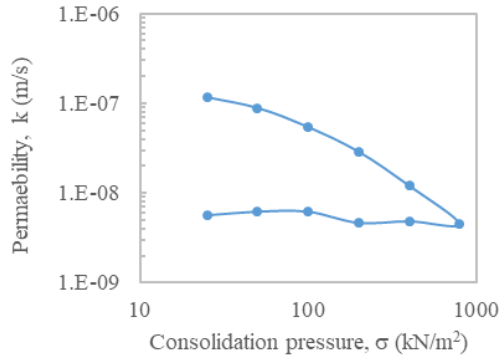

(a) Overburden dependency in permeability

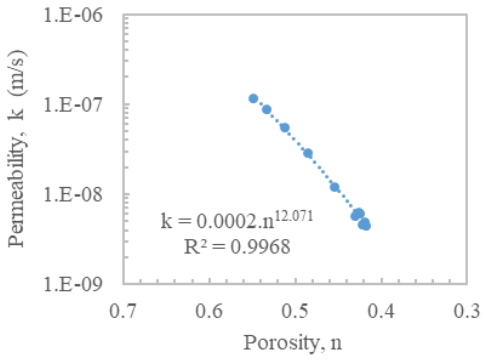

(b) Porosity dependency in permeability

Fig. 10 Falling head permeability tests of saturated zeolite

higher values of σ'_v. Fig. 9(a) illustrates that the normalized values calculated for inundated samples were lower than the values of dry samples. In addition, the reduction in shear strength values due to inundation was calculated to be limited to a range of 12% under the relevant stress levels, as shown in Fig. 9(b).

4.3 Permeability tests

The change in the hydraulic conductivity of the inundated zeolite column with depth was studied by performing falling head-type permeability tests in a specialized oedometer cell at stress levels between 25 and 800 kN/m². Fig. 10(a) shows the apparent reduction in k_v with σ'_v. Note that, after 800 kN/m², the observed values of k_v during unloading stages were almost constant due to the limited swelling potential, as shown in Fig. 5. The sample volume was kept constant throughout the test, therefore, the k_v value observed at each stress level can be interpreted in the context of the determined n values attained after the end of the primary consolidation or primary swelling. Fig. 10(b) illustrates the proportional relationship between the coefficients of k_v and n.

The bench-scale PRB system was used to approximate the initial hydraulic conductivity of the reactive media composed of dry zeolite, and sand. The permeability coefficient of each medium was required as an input for the 2D flow analysis of the bench-scale model, therefore, constant head-type permeability tests were also conducted on sand samples. The permeability coefficient of the sand prepared at the same relative density used in the model was determined as 2.5 10^{-5} m/s under the relevant hydraulic gradient conditions.

After the designated total head difference was measured between the inlet and outlet sides, the discharge volume of water through the vertical zeolite barrier was recorded by time. The average total discharge was observed to be 2.15 10^{-7} $m^3/s/m$, after a water volume equivalent to more than 11 times the zeolite pore volume had passed through the barrier.

5. Numerical analysis

In the study, a numerical model was proposed to calculate the compression of the dry zeolite column during the filling and wetting stages. Initially, the compression by self-weight loading along the fill height of the loose state dry zeolite column was numerically solved – this quantity was calculated for a unit volume of fill using compression ratio versus vertical pressure plots, as shown in Fig. 6(a). Fig. 11 presents the proposed model used for calculating the compression of a dry zeolite column composed of (m+1) number of identical elements, where h is the height and γ_d is the initial dry unit weight in the loose state. The height of each element decreases as it is subjected to increasing overburden pressure; this

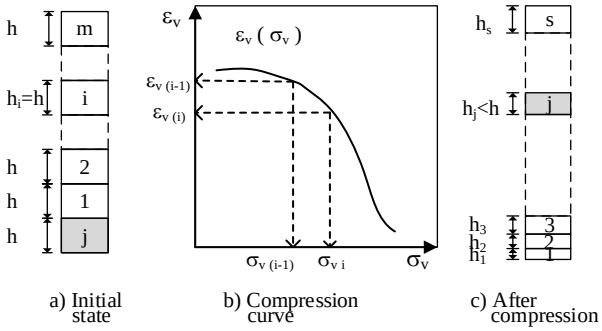

Fig. 11 Numerical modelling of self-loading of reactive column

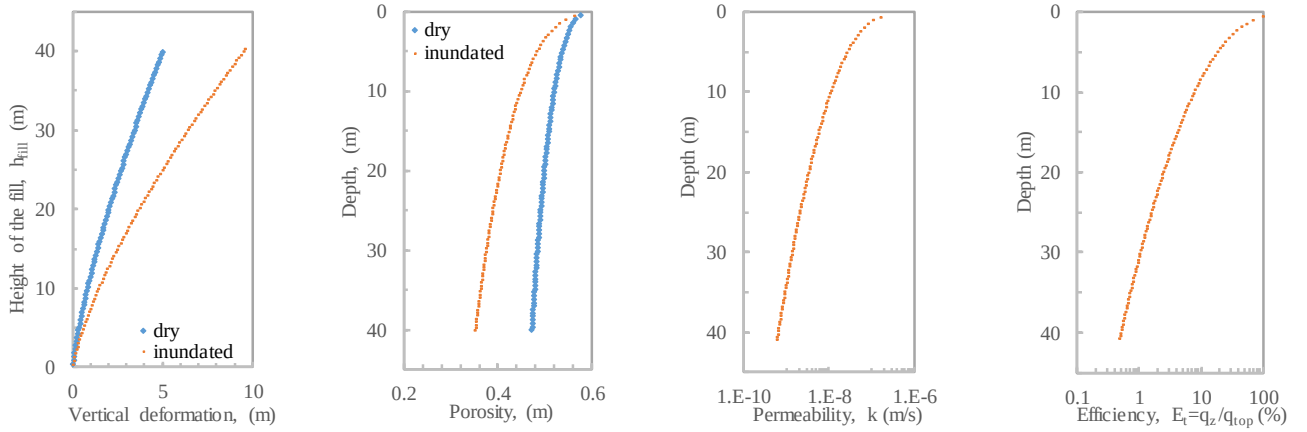

(a) Self-load compression of zeolite column

(b) Porosity throughout the zeolite column

(c) Vertical permeability throughout the zeolite column

(d) Discharge efficiency throughout the zeolite column

Fig. 12 1D Numerical modeling of zeolite column

behavior is shown for the j^{th} element in Fig. 11(a), which is overlain by m elements, where the value of σ_v is given by Eq. (1).

$$\sigma_v = \sum_{i=1}^{m} \gamma_d \cdot h_i \tag{1}$$

At the final fill height, the vertical strain of an element is equal to the sum of the strains caused by each of the loading increments shown in Fig. 11(a). A stress-strain function, as observed in Fig. 6(b), is applicable to determine the amount of compression of an element at any stress interval, as shown in Fig. 11(b). Thus, the final height of the element was calculated using Eq. (2).

$$h_j = \sum_{i=1}^{m} h \cdot \left[1 - \left(\varepsilon_v\left(\sigma_{v_i}\right) - \varepsilon_v\left(\sigma_{v_{(i-1)}}\right)\right)\right] \tag{2}$$

The cumulative vertical strains of the elements have a significant impact on the mass of reactive material required to achieve the necessary barrier height. Therefore, the same procedure adopted for the j^{th} element in Fig. 11(a) must be repeated for a number of elements, s, which is shown in Fig. 11(c) after compression. A trial and error method was used to define the exact number of elements required to achieve a fill height equal to h_{fill} in Eq. (3).

$$h_{fill} = \sum_{j=1}^{s} h_j \tag{3}$$

However, the wetting-induced swell or collapse behavior of the reactive column will affect the performance of the barrier. Therefore, in the model, hydro-compression was taken into account considering the height and overburden pressure of each element separately after dry compression. The relevant hydro-compression ratio was taken from the function given in Fig. 6(c) and the final height of the column h_{final} is calculated using Eq. (4).

$$h_{final} = \sum_{j=1}^{s} h_{j_{inundated}} \tag{4}$$

The calculated h_{final} should be equal to the height of the barrier in the design. To accomplish this, several trials are required to account for the amount of wetting-induced swell or collapse of the dry reactive material subjected to overburden pressure. In this preliminary study, the total vertical displacements of the elements calculated to satisfy a fill height of zeolite column were presented cumulatively for a reactive barrier of 40.0 m height, both before and after

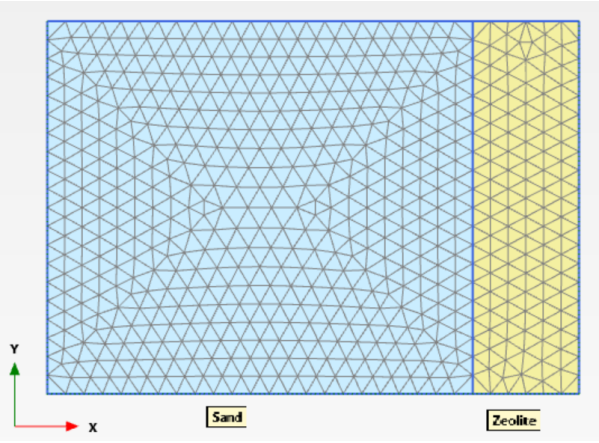

(a) Finite element mesh of zeolite column with sand environment

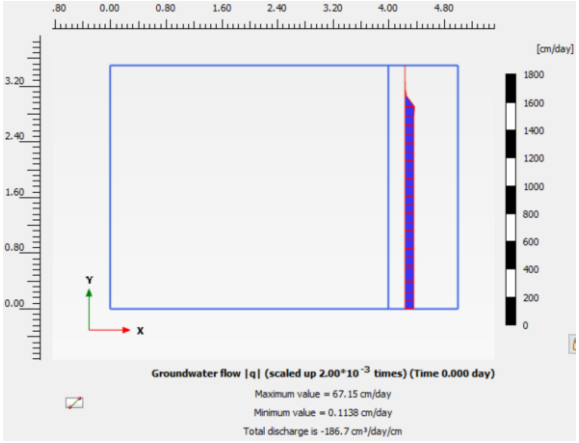

(b) Groundwater flow within the zeolite media

Fig. 13 2D flow analysis of bench scale model

inundation, without a cover cap (Fig. 12(a)). As an example, the required amount of material for a 20 m high reactive barrier after inundation could be supplied by a 24 m zeolite column in a loose and dry state. In addition, the values of n calculated throughout a 40.0 m high barrier are plotted in Fig. 12(b), which illustrates the amount of reduction due to the overburden pressure before and after inundation. Based on the n versus k_v relationship observed for saturated zeolite samples (Fig. 10(b)), the calculated k_v versus depth plots show an apparent reduction with depth (Fig. 12(c)). Consequently, this indicates a reduction in transportation efficiency with depth, as defined by the ratio of the transported volume of water through a unit volume of reactive material located at any depth (Fig. 12(d)).

The design of permeable barrier technology can be optimized through the application of 2D or 3D numerical analysis software. Flow models using the finite element or finite difference numerical methods will accept separate vertical and horizontal permeability values, where these values differ. The findings of the bench-scale studies can be used to calibrate the input parameters of the numerical models to improve evaluations of the performance and longe vity scenarios for the PRB. Fig. 13(a) presents a 15-node 2D finite element fine mesh used for modeling the bench-scale test. Flow analysis was conducted using a constant head assumption at both permeable influent and effluent boundaries, while the bottom boundary of the model was set as impermeable. While the horizontal permeability coefficient k_h of sand was assumed to be equal to k_v for modeling purposes, the k_h of zeolite was expected to differ from the k_v value assigned based on the observations of vertical permeability tests. Therefore, this parameter was set to be the same as the total discharge value, observed in the bench-scale tests (Fig. 13(b)), i.e., the k_h of zeolite was assumed to be as 6.37×10^{-6} m/s.

6. Discussion

The technology required for the treatment of contaminated groundwater requires hydrogeological analysis in terms of both the hydraulic conductivity of the layers and the stress conditions within the soil profile. Groundwater flow analysis for the treatment in PRB applications must also be defined for the stress conditions after construction, as the emplacement methodology may have a crucial effect on the in situ conditions. This study mainly focuses on the use of tremie tubes for dry filling of reactive material in the trench box of a funnel and gate-type PRB keyed into a competent aquitard-type vertical PRB. The calculation of lateral pressure acting on the temporary or permanent sidewalls of the trench box also requires the shear strength of the reactive material to be determined, which may change during the construction period or even afterward. In the scope of this study, the direct shear tests, performed under a range of σ_v values representing the entire fill depth of a 40 m zeolite barrier, indicated that the shear strength of dry zeolite decreased by 8% after inundation. Thus, the shear strength of zeolite in the inundated case was found to be more critical compared to the case of dry fill in the trench. Therefore, a pre-hydration approach is proposed to limit the wetting-induced reduction in shear strength during active use of the PRB.

Pre-hydration has a known beneficial effect in lowering the permeability of clays when used in impervious barriers, especially for montmorillonite-based soils that have high osmotic swelling potential (Gueddouda *et al.* 2010). However, in the long-term, the flow of contaminated groundwater through the barrier aggregates the jelly structure by cation exchange around the clay platelets, which may increase the permeability. The decreased pollutant retention time in the reactive medium before the calculated breakthrough point leads to failure of the barrier. Conversely, in PRB implementations the use of reactive material with a negligible swelling potential presents the effects of pre-hydration by decreasing the permeability due to wetting induced collapse. Besides, the effect of long-term changes in permeability on performance of PRBs should be studied based on the type of the reactive material.

Artificially produced clay balls, organoclays and hyper clays (Rajapakse *et al.* 2015, Di Emidio *et al.* 2015,

Bagherifam *et al*. 2021) can be used regarding the flow conditions in a barrier, however, the use of raw reactive materials which are available on-site will tend to be more economical. The naturally occurring zeolite clinoptilolite is one of the alternative reactive materials proposed for use in PRB implementations that exhibits low values of swelling and plasticity indexes.

The porosity of the reactive material used in the batch tests should be well-defined to model the in situ conditions. The compressibility of the material should be tested taking into account the emplacement methodology and inundation. The man-made compaction performed in the trench box of a PRB will tend to increase construction costs, and may lead to health issues related to potential leakage caused by improper compaction. This approach is also not practically possible for barriers with large heights. Therefore, the use of tremie tubes may be applicable if the in situ conditions of the zeolite column are well defined. The self-loading compression through the zeolite column requires higher compression ratios with depth under the effects of increased overburden pressure to be observed, as shown in this study. The effect of hydration on dry-filled reactive column material should be observed through swell or collapse tests. In this study, the hydro-compression ratio observed after inundation increases proportionally to the overburden pressure, therefore, the wetting-induced final values of n must be taken into account for assessment of the barrier performance. Fig. 6(a) illustrates that the compression curve of pre-hydrated zeolite samples is suitable for modeling the compression behavior of dry zeolite samples after inundation up to values of 300 kN/m^2. Considering the insignificant amount of free swelling observed, consistent with the literature (Aksoy 2010), the wetting during the filling process is noted to accelerate the wetting-induced hydro-compression behavior with only limited adverse effects on the shear strength of the zeolite column. Therefore, the wetting-induced collapse of dry-filled zeolite columns could be employed before installation of the final impervious cap cover to prevent further hydro-compression behavior caused by transient flow conditions during the service life of the barrier, which would affect the performance of the PRB.

The change in the n value of the reactive media after inundation could be tested to reveal the reduction in permeability of the PRB systems. The compression curves of the saturated reactive material, as presented for zeolite in Fig. 7, are applicable to predict the settlement amount of the column during the lifespan of the barrier by using the C_c and C_α values observed in consolidation tests. In addition, the permeability tests conducted on the samples prepared at different porosities can be used to illustrate the proportional relationship between n and k_v. However, the importance of the stress history on k_v can also be calculated by the permeability tests conducted in a special oedometer cell, such as the one used in this study. The increase in permeability in the case of the decrease in the effective stress, such as high water level conditions, can also be examined at predesignated stress levels by unloading, as shown in Fig. 10, which were observed to be limited for zeolite after 800 kN/m^2. The low value of swelling index, in addition to the limited change in permeability during the unloading stages, show that the vacuum preloading method may be applicable against the effects of an increase in the effective stress such as low water level conditions. However, the magnitude of preloading should be designed with caution as an incorrect reduction in the permeability of the zeolite column may cause the contaminated groundwater to bypass the barrier.

The bulk density of zeolite along the depth of the reactive column is important to determine the porosity, which is one of the key factors controlling permeability. The post-construction permeability values of the reactive column with depth can be calculated by use of k_v versus n plots, determined from falling head permeability tests combined with 1D consolidation tests. Thus, a 1D numerical model was proposed for calculation of the compression behavior of the reactive material due to self-loading, in which dry emplacement was assumed to initially be in the loosest state. In this model, compression curves of the swell or collapse tests were used to determine the n versus depth plots for the post-construction stage. The calculated n values were then matched with those obtained from the falling head permeability test to predict the reduction in permeability along the zeolite column. Comparing the change in discharge capacity at depth with the top of the column, the discharge efficiency of zeolite was observed to decrease with depth; the discharge efficiency decreased to less than 2% when the column was 20 meters or longer.

The assumptions used to simplify the problem for modeling may not accurately simulate the in situ PRB conditions, thus, bench-scale tests are required to verify the model parameters of 2D or 3D groundwater flow analysis. The bench-scale model shown in Fig. 5 was previously modified to propose a treatment technology for surficial water and groundwater contaminated by radionuclides in waste storage areas using the PRB system (Camtakan 2021). Cevikbilen and Camtakan (2020), discussed the preliminary findings on the hydraulic conductivity of double layer barrier composed of zeolite and sepiolite prior to the contamination of cesium for a modified setup of the model. The observations from the bench-scale test used in this study reveal that the total discharge of the 2D finite element flow analysis can only be verified if the horizontal permeability of the zeolite was sufficiently higher than the vertical permeability values observed in the laboratory testing. Practically, the numerical models use a parameter c_k, defined in Eq. (5), to represent the change of the permeability coefficient from an initial value of k_0 to a final value of k in a soil layer, considering the change in the void ratio Δe.

$$c_k = \frac{\Delta e}{\log\left(\frac{k}{k_0}\right)} \tag{5}$$

In PRB implementations, the c_k parameter can represent the variation in permeability with depth in the zeolite column when a gravity loading calculation is applied that results in different values of Δe for reactive material with depth. According to the falling load tests, the zeolite

c_k value is observed to vary within a narrow range between -0.22 and -0.31, which gradually increases with overburden pressure. However, the validity of the calculated c_k values in determining the change in horizontal permeability is controversial. Therefore, as a proposed future study, it would be appropriate to establish a new bench-scale model that can simulate horizontal flow conditions at different overburden pressures to reveal the directional dependence in the permeability of the zeolite used as a reactive material in PRB.

7. Conclusions

This study evaluates the use of laboratory testing of locally available zeolite reactive materials for optimizing the design of PRBs using geotechnical modeling. It also emphasizes the benefits of the mechanical testing on reactive materials prior to the construction stage since they provide some of the numerical model parameters essential to adjust the performance of PRB with depth. The results of one dimensional compression, shear strength and permeability tests were discussed to develop the bench-scale model used for PRBs. The change in the geotechnical properties of dry zeolite during emplacement was revealed through a combination of laboratory testing and numerical modeling.

It is also suggested that the sustainability of PRB technology will be improved when the local raw materials are available as the reactive source that will reduce the initial and maintenance costs. Beside to the environmental studies, mainly focused on the reactivity of the material for a site specific pollutant, the change in hydraulic conductivity of the material should be controlled by considering its dry or wet emplacement and the stress strain conditions along the depth of the barrier.

- The hydration of the dry zeolite emplaced in the trench before cap construction will limit the loss of strength and the effects of hydro-compression due to further transient flow conditions.
- The self-weight consolidation behavior of the inundated zeolite column presents a decreasing discharge efficiency with depth. Practically, extending the barrier height more than 20 m will be inefficient with a loss of 98% in the hydraulic performance compared to the top.
- The importance of bench-scale tests is emphasized for calibrating model parameters in 2D numerical flow analysis.
- It should be noted that additional tests are required to simulate the long-term stability and performance of barriers with site-specific pollutants.

Acknowledgments

This study was funded by Istanbul Technical University Research Fund (ITÜ-BAP; project no MGA-43814) The author would like to thank the ITU, Faculty of Civil Engineering, Geotechnical Engineering Laboratories. MATLAB R2018a tools were used to model 1D self–loading and hdyro-compression analysis of zeolite column. PLAXIS 2D (2019) software was used to model 2D flow analysis of bench scale test. Generic Mapping Tools (GMT; Wessel and Smith,1998) software was used to prepare Fig. 1. The author appreciates Dr. Zeynep Camtakan for supporting in bench scale model setup used in this study.

References

Aksoy Y.Y. (2010), "Characterization of two natural zeolites for geotechnical and geoenvironmental applications", *App. Clay Sci.*, **50**(1), 130-136. https://doi.org/10.1016/j.clay.2010.07.015.

ASTM D854 (2014), Standard Test Methods for Specific Gravity of Soil Solids by Water Pycnometer, ASTM Int., West Conshohocken, PA, USA.

ASTM D2434 (2019), Standard Test Method for Permeability of Granular Soils (Constant Head), ASTM Int., West Conshohocken, PA, 2019, USA.

ASTM D2435 (2020), Standard Test Methods for One-Dimensional Consolidation Properties of Soils Using Incremental Loading, ASTM Int., West Conshohocken, PA, USA.

ASTM D2487 (2017), Standard Practice for Classification of Soils for Engineering Purposes (Unified Soil Classification System), ASTM Int., West Conshohocken, PA, USA.

ASTM D3080 (2011), Standard Test Method for Direct Shear Test of Soils Under Consolidated Drained Conditions, ASTM Int., West Conshohocken, PA, USA.

ASTM D4253 (2016), Standard Test Methods for Maximum Index Density and Unit Weight of Soils Using a Vibratory Table, ASTM Int., West Conshohocken, PA, USA.

ASTM D4254 (2016), Standard Test Methods for Minimum Index Density and Unit Weight of Soils and Calculation of Relative Density, ASTM Int., West Conshohocken, PA, USA.

ASTM D4546 (2021), Standard Test Methods for One-Dimensional Swell or Collapse of Soils, ASTM Int., West Conshohocken, PA, 2021, USA.

ASTM D5890 (2019), Standard Test Method for Swell Index of Clay Mineral Component of Geosynthetic Clay Liners, ASTM Int., West Conshohocken, PA, USA.

ASTM D6913 (2017), Standard Test Methods for Particle-Size Distribution (Gradation) of Soils Using Sieve Analysis, ASTM Int., West Conshohocken, PA, USA.

ASTM D7928 (2021), Standard Test Method for Particle-Size Distribution (Gradation) of Fine-Grained Soils Using the Sedimentation (Hydrometer) Analysis, ASTM Int., West Conshohocken, PA, USA.

Bagherifam, S., Brown, TC., Fellows, CM. Naidu, R. and Komarneni, S. (2021), "Highly efficient removal of antimonite (Sb (III)) from aqueous solutions by organoclay and organozeolite: Kinetics and Isotherms", *App. Clay Sci.*, 203. https://doi.org/10.1016/j.clay.2021.106004 .

Bone, B.D. (2012), "Review of UK guidance on permeable reactive barriers", *Peoceedings of the Taipei Int. Conf. on Remediation and Mgmt. of Soil and Groundwater Contaminated Sites*, Taipei, Taiwan, October.

Bowles M.W., Bentley L.R., Hoyne B. and Thomas D.A. (2000), "In situ ground water remediation using the trench and gate system", *Ground Water*, **38**(2) 172-181. https://doi.org/10.1111/j.1745-6584.2000.tb00328.x.

Camtakan, Z. (2021), "Investigation of the treatment of cesium in waste storage areas with the permeable reactive barrier (PRB) system", Ph.D. Dissertation, Ege University, Izmir.

Cevikbilen, G. and Camtakan, Z. (2020), "Bench-scale studies of a permeable reactive barrier system for radiocesium removal", *European Geoscience Union General Assembly*, Online, May.

Di Emidio, G., Flores, RDV, Scipioni, C, Fratalocchi, E, Bezuijen, A. (2015) "Hydraulic and mechanical behaviour of cement-

bentonite mixtures containing HYPER clay: impact of sulfate attack", *Proceedings of the 6th Int. Symp. on Deformation Characteristics of Geomaterials",* Buenos Aires, Argentina, November.

Gavaskar, A.R. (1999), "Design and construction techniques for permeable reactive barriers", *J. Hazardous Mater.*, **68**(1-2), 41-71. https://doi.org/10.1016/S0304-3894(99)00031-X.

Ghiyas, S.M.R. and Bagheripour, M.H. (2020) "Stabilization of oily contaminated clay soils using new materials: Micro and macro structural investigation", *Geomech. Eng.*, **20**(3) 207-220. https://doi.org/10.12989/gae.2020.20.3.207.

Gueddouda, M.K., Lamara, M., Abou-bekr, N. and Taibi, S. (2010), "Hydraulic behavior of dune sand-bentonite mixtures under confining stress", *Geomech. Eng.*, **2**(3), 213-227, https://doi.org/10.12989/gae.2010.2.3.213.

Henderson A.D. and Demond A.H. (2007), "Long-term performance of zero-valent iron permeable reactive barriers: A critical review", *Environ. Eng. Sci.*, **24**(4). https://doi.org/10.1089/ees.2006.0071.

IAEA-TECDOC-1088 (1999), Technical Options for the Remediation of Contaminated Groundwater, Int. At. Energy Agency, Vienna, Austria. https://www.pub.iaea.org/MTCD/publications/PDF/te_1088_prn.pdf.

ITRC (2005), Permeable reactive barriers: Lessons learned/new directions. PRB-4. Interstate Technology & Regulatory Council, Permeable Reactive Barriers Team. Washington, D.C. www.itrcweb.org.

Joseph A.S. and Varghese M. (2017), "Study on amended landfill liner using bentonite and zeolite mixtures", *Int. Res. J. of Eng. Tech.*, **4**(4), 1130-1133. https://www.irjet.net/archives/V4/i4/IRJET-V4I4232.pdf .

Kayabalı, K. and Kezer, H. (1998), "Testing the ability of bentonite amended zeolite (clinoptilolite) to remove heavy metals from liquids waste", *Env. Geology*, **34**, 95-102. https://doi.org/10.1007/s002540050259.

Korte, N.E. (2001), "Zero-Valent Iron Permeable Reactive Barriers: A Review of Performance. United States" Environ. Sciences Division Pub. No. 5056, U.S. Department of Energy, Washington DC. https://doi.org/10.2172/814389.

Kütük, A.C., Yüksel, M., Sözüdoğru, S., Ömer, F. Kayabah, İ. (1996), "Gördes zeolitli (klinoptilolit) tüflerinin mineralojisi ve bitki yetiştirme ortamında kullanımı", Jeoloji Mühendisliği **48**, 32-39.

Ludwig, R.D., McGregor, R.G., Blowes, D.W., Benner, S.G. and Mountjoy, K. (2005), "A permeable reactive barrier for treatment of heavy metals", *Ground Water* **40**(1), 59-66. https://doi.org/10.1111/j.1745-6584.2002.tb02491.x.

Mesri, G. (1973), "Coefficient of secondary compression", *ASCE J. Soil Mech. Found. Div.*, **99**(1), 123-137. https://doi.org/10.1061/JSFEAQ.0001840.

Morrison, S.J., Naftz, D.L., Davis, J.A. and Fuller, C.C. (2003), "Chapter 1 - introduction to groundwater remediation of metals, radionuclides, and nutrients with permeable reactive barriers", (Eds., David L. Naftz, Stan J. Morrison, Christopher C. Morrison S.J., Naftz D.L., Davis J.A., Fuller C.C.), *Handbook of Groundwater Remediation using Permeable Reactive Barriers*, Academic Press, 1-15.

MTA (2021), Zeolite resources in Turkey; MTA, Ankara, Turkey. www.mta.gov.tr/v3.0/sayfalar/hizmetler/images/b_h/ zeolit.jpg .

Naidu, R. and Birke, V. (2015), *Permeable Reactive Barrier: Sustainable Groundwater Remediation*, CRC Press Taylor & Francis Group, Boca Raton, FL, USA.

Navarro, A., Chimenos, J.M., Muntaner, D. and Fernández, A.I. (2006), "Permeable reactive barriers for the removal of heavy metals: Lab-scale experiments with low-grade magnesium oxide", *Groundwater Monit. Remediation*, **26**(4), 142-152. https://doi.org/10.1111/j.1745-6592.2006.00118.x.

Oren, A.H. and Kaya, A. (2014) "Compaction and volumetric shrinkage of bentonitic mixtures", *Proc. of the Inst. of Civil Eng. Geot. Eng.*, **167**(1), 51-61. https://doi.org/10.1680/geng.11.00043.

Oren, A.H., Kaya, A. and Kayalar, A.S. (2011), "Hydraulic conductivity of zeolite–bentonite mixtures in comparison with sand–bentonite mixtures", *Canadian Geot. J.*, **48**(9), 1343-1353. https://doi.org/10.1139/t11-042.

Ören, A.H. and Özdamar, T. (2013), "Hydraulic conductivity of compacted zeolites", *Waste Mgmt. Res.*, **31**(6), 634-640. https://doi.org/10.1177/0734242X13479434.

Park, J.B., Lee, S.H., Lee, J.W. and Lee, C.Y. (2002), "Lab scale experiments for permeable reactive barriers against contaminated groundwater with ammonium and heavy metals using clinoptilolite (01-29B)", *J. Hazardous Mater.*, **95**(1-2), 65-79. https://doi.org/10.1016/S0304-3894(02)00007-9.

Powell, R.M., Puls, R.W., Blowes, D.W., Vogan, J.L., Gillham, R. W., Powell, P.D., Schultz, D. Landis, R. and Sivavec, T. (1998), "Permeable reactive barrier technologies for contaminant remediation", *U.S. Environ. Protection Agency*, Washington, D.C., EPA/600/R-98/125 (NTIS 99-105702).

Rajapakse, J.P., Gallage, C., Dareeju, B., Madabhushi, G. and Fenner, R. (2015), "Strength properties of composite clay balls containing additives from industry wastes as new filter media in water treatment", *Geomech. Eng.*, **8**(6), 859-872. https://doi.org/10.12989/gae.2015.8.6.859.

Smith, W.H.F. and Sandwell, D.T. (1997a), "Measured and estimated seafloor topography (version 4.2) ", World Data Centre-A for Marine Geology and Geophysics research publication RP-1, poster, 34″ × 53″.

Smith, W.H.F. and Sandwell, D.T. (1997b), "Global seafloor topography from satellite altimetry and ship depth soundings", *Science*, **277**, 1957-1962.

Smyth, D. (1995), University of Waterloo Research Efforts, Remediation Technologies Development Forum, Permeable Barriers Work Group, Meeting Summary, Wilmington, Delaware USA, May.

Thiruvenkatachari, R., Vigneswaran, S. and Naidu, R. (2008), "Permeable reactive barrier for groundwater remediation", *J. Ind. Eng. Chem.*, **14**(2), 145-156. https://doi.org/10.1016/j.jiec.2007.10.001.

Tuncan, A., Tuncan, M., Koyuncu, H. and Guney, Y. (2003), "Use of natural zeolites as a landfill liner", *Waste Mgmt. Res.: The J. for a Sust. Circ. Econ.*, **21**(1), 54–61. https://doi.org/10.1177/0734242X0302100107.

USEPA (2002), "Field applications of in-situ remediation technologies: Permeable reactive barriers", *Office of Solid Waste and Emergency Response Technology Innovation Office*, Washington, DC.

Villalobos, F.A., Leiva, E.A., Jerez, Ó. and Poblete, M.E. (2018), "Experimental study of the fine particles effect on the shear strength of tuff zeolites", *J. Const.*, **17**(1), 23-37. https://doi.org/10.7764/RDLC.17.1.23.

Vignola, R., Bagatina, R., D'Auris, A.F., Flego, C., Nalli, M., Ghisletti, D., Millini, R. and Sisto, R. (2011), "Zeolites in a permeable reactive barrier (PRB): One year of field experience in a refinery groundwater—Part 1: The performances", *Chem. Eng. J.*, **178**, 204-209. https://doi.org/10.1016/j.cej.2011.10.050.

Walker, K.L. Jr., McGuire, T.M., Adamson, D.T. and Anderson, R. H. (2020), "Long-term evaluation of mulch biowall performance to treat chlorinated solvents", *Groundwater Monit. Remediation*, **40**(1), 35-46. https://doi.org/10.1111/gwmr.12364.

Wang, C.B. and Zhang, W.X. (1997), "Synthesizing nanoscale iron particles for rapid and complete dechlorination of TCE and PCBs", *Environ. Sci. Technol.*, **31**(7) 2154-2156. https://doi.org/10.1021/es970039c.

Wessel, P. and Smith, W.H.F. (1998), "New, improved version of the Generic Mapping Tools released", EOS Trans. Am. Geophys. Union 7.

Widomski, M.K., Musz-Pomorska, A. and Franus, W. (2021), "Hydraulic and swell–shrink characteristics of clay and recycled zeolite mixtures for liner construction in sustainable waste landfill", *Sustainability*, **13**(13), 7301. 1-20. https://doi.org/10.3390/su13137301.

GC

Appendix

Table A.1 Chemical Composition of zeolite (DIN51001) (taken from https://zeoproducts.com/assets/catalogues/tech_data_sheet/en/zeo_oil.pdf)

	w/w (%)		w/w (%)		w/w (%)
SiO_2	68.8	TiO_2	0.08	Na_2O	0.72
Al_2O_3	14.6	CaO	2.57	K_2O	3.43
Fe_2O_3	0.91	MgO	0.63	SiO_2/Al_2O_3	4.7

Table A.2. Physical and Chemical Properties of Zeolite samples (taken from https://zeoproducts.com/assets/catalogues/tech_data_sheet/en/zeo_oil.pdf)

Properties	Value
Surface Area (m^2/g)	40.79
NH4+ Change Capacity (meq/g)	1.6-2.0
Thermal Stability	Up to 840°C
Water Retention Capacity (%)	35-40